

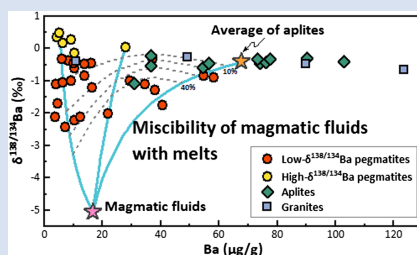
# Barium isotope evidence for a magmatic fluid-dominated petrogenesis of LCT-type pegmatites

G. Deng<sup>1</sup>, D. Jiang<sup>1,2</sup>, G. Li<sup>3</sup>, Z. Xu<sup>3</sup>, F. Huang<sup>1,2\*</sup>



<https://doi.org/10.7185/geochemlet.2426>

## Abstract



Understanding the petrogenesis of granitic pegmatites associated with Li mineralisation is fundamental in constraining rare metal enrichment mechanisms. However, there is still significant controversy surrounding the central issue of the nature of pegmatite-forming liquids. Here, we report Ba isotope data for a 3000 m borehole in the Jiajika pegmatite field that hosts the largest hard rock-type Li deposit in Asia. The pegmatites exhibit markedly lower  $\delta^{138/134}\text{Ba}$  than the wall rocks and the average upper continental crust, which cannot be attributed to low degree anatexis of metasedimentary or crystal fractionation of highly evolved granitic magmas. Instead, modelling suggests that their low  $\delta^{138/134}\text{Ba}$  most likely results from substantial involvement (10–40 %) of isotopically light hydrothermal fluids exsolved from the underlying magmatic reservoirs. In the context of transcrustal magmatic system, these magmatic fluid components may be a key medium in extracting, concentrating, and transporting Li to provide a material source for mineralisation in granitic pegmatites.

Received 17 March 2024 | Accepted 3 June 2024 | Published 28 June 2024

## Introduction

Granitic pegmatites are granitoids with characteristic textures and constitute one of the most important sources of rare metal elements (London, 2018). The Li-Cs-Ta (LCT) pegmatites, as a type of Li deposit with high grade and wide distribution (Fig. 1a), supply approximately half of global Li production and are the main target of future exploration (Benson *et al.*, 2017). Exploring the petrogenesis of LCT-type granitic pegmatites is thus crucial for understanding the enrichment mechanisms of Li and other rare metals.

Most LCT-type pegmatites are considered to be the product of extreme differentiation of granitic magmas (Thomas and Davidson, 2016; London, 2018). However, the nature of the pegmatite-forming liquids, especially with regard to the role of H<sub>2</sub>O and fluxing elements (*e.g.*, B, F, and P), is still highly controversial. The constitutional zone refining model, based mainly on experimental petrology, large scale whole rock analyses, and simulations, suggests that the initial pegmatite-forming liquids are essentially granitic melts inherited from the parental magmas (London, 2018). Incompatible components, including H<sub>2</sub>O, fluxing elements, and rare metals, are continuously enriched in a boundary layer liquid adjacent to the crystallisation front (London, 2014). In this scenario, H<sub>2</sub>O and fluxing elements only play a role in locally lowering viscosity and increasing elemental diffusivity, with aqueous fluid considered unnecessary or even unlikely. In contrast, an alternative model, based mainly on the studies of melt and fluid inclusions, proposes that the formation

of LCT-type pegmatites begins with single phase supercritical fluids resulting from miscibility of magmatic fluids and silicate melts (Thomas and Davidson, 2016). These supercritical fluids can acquire very high initial water and rare metal contents from granitic source magmas, followed by phase separation after emplacement that further enriches Li in the H<sub>2</sub>O-rich melt/fluid phase (Thomas *et al.*, 2019). Numerous attempts have been made to distinguish between the two models (Zhang *et al.*, 2021; Troch *et al.*, 2022), yet a consensus remains elusive.

Barium (Ba) is fluid-mobile and compatible during the crystallisation of granitic magmas. Recent studies highlight the great potential of Ba isotopes in distinguishing between crystal fractionation and magmatic fluid effect. The near eutectic composition of granitic pegmatites implies that K-feldspar controls the Ba budget of the crystalline mineral assemblage, which could result in significantly higher  $\delta^{138/134}\text{Ba}$  (defined as  $[(^{138}\text{Ba}/^{134}\text{Ba})_{\text{sample}} / (^{138}\text{Ba}/^{134}\text{Ba})_{\text{NIST3104a}} - 1] \times 1000$  (‰)) in the residual melts (Deng *et al.*, 2021). Conversely, as magmatic fluids are experimentally demonstrated to preferentially incorporate light Ba isotopes relative to silicate melts (Guo *et al.*, 2020), their substantial involvement would dramatically reduce  $\delta^{138/134}\text{Ba}$  of the pegmatite systems (Huang *et al.*, 2021; G. Deng *et al.*, 2022). Hence, Ba isotopes offer a powerful tool for deciphering the nature of pegmatite-forming liquids.

Here, we present high precision Ba isotope data for a suite of borehole samples from the Jiajika granitic pegmatite field (eastern Tibetan Plateau). This pegmatite field is formed within the Jiajika gneiss dome that has a two-mica granite core, mantled

1. State Key Laboratory of Lithospheric and Environmental Coevolution, School of Earth and Space Sciences, University of Science and Technology of China, Hefei 230026, Anhui, China  
2. CAS Center for Excellence in Comparative Planetology, USTC, Hefei 230026, Anhui, China  
3. State Key Laboratory for Mineral Deposits Research, School of Earth Sciences and Engineering, Nanjing University, Nanjing 210023, China  
\* Corresponding author (email: [fhuang@ustc.edu.cn](mailto:fhuang@ustc.edu.cn))

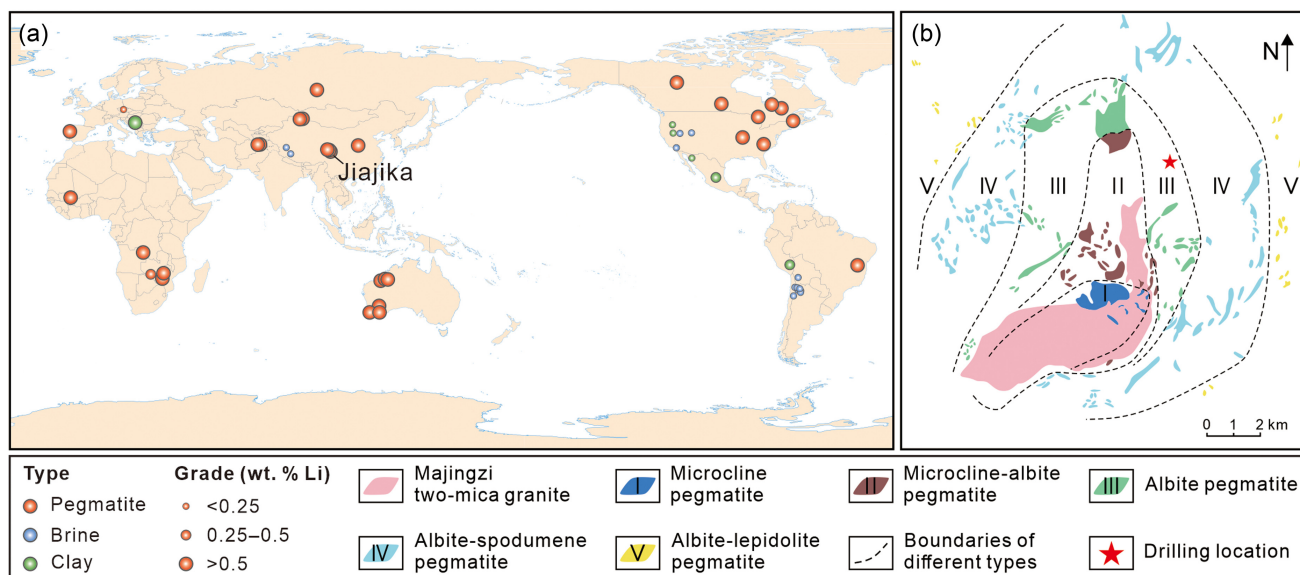


**Figure 1** (a) Location and grades of representative pegmatite, brine, and clay Li deposits worldwide. See data sources in Table S-1. (b) Simplified geological map of the Jiajika pegmatite field (modified after Zhao *et al.*, 2022).

by a succession of metasedimentary rocks. More than 500 LCT-type pegmatite veins are spatially zoned around the two-mica granite, in the order from the pluton outward: microcline pegmatite (I), microcline-albite pegmatite (II), albite pegmatite (III), albite-spodumene pegmatite (IV), and albite-lepidolite pegmatite (V) (Fig. 1b). The Li mineralisation is mainly developed within zones IV and V, as well as some veins in zone III, with total estimated Li<sub>2</sub>O reserves of up to 3.0 Mt, ranking the first in Asia (Huang *et al.*, 2020). The studied samples were collected from different depths of a borehole of 3211.21 m, which consists of 35 % metasediments, 14 % granite-aplites, and 51 % pegmatites (Fig. 2a) (Xu *et al.*, 2023). Spodumene-bearing pegmatites are only observed at depths between 0 and 100 m, while deeper pegmatites correspond to surface zones I and II pegmatites without Li mineralisation (Wang *et al.*, 2023). Detailed geological background and sample description are available in the Supplementary Information. Due to their proximity to the buried main part of the parental granite compared to samples collected from the surface, these borehole samples may provide a strong documentation of the initial compositional characteristics of the pegmatite system. Our results show extremely low  $\delta^{138/134}\text{Ba}$  of pegmatites, supporting a comprehensive influence of magmatic fluids on their compositions, and thus a possible key role in rare metal enrichment.

## Results

The Ba isotope analytical method is detailed in the Supplementary Information. The long-term external precision for  $\delta^{138/134}\text{Ba}$  is better than 0.05 ‰ (2 s.d.). The  $\delta^{138/134}\text{Ba}$  of rock standards agree with published values, and the results of replicates are consistent within error (Table S-2), demonstrating the reliability of our data.

There are significant variations in  $\delta^{138/134}\text{Ba}$  of the borehole samples (Fig. 2). Overall, pegmatites have the lowest Ba contents (3.7–130.2  $\mu\text{g/g}$ , mostly <50  $\mu\text{g/g}$ ) and the largest range of  $\delta^{138/134}\text{Ba}$  (–2.44 to +0.47 ‰) among the four sample types. Notably, their  $\delta^{138/134}\text{Ba}$  does not show a systematic variation with depth. Granitic aplites and granites have moderate and less variable Ba contents (30.9–102.9  $\mu\text{g/g}$  and 11.0–123.8  $\mu\text{g/g}$ , respectively) and narrower  $\delta^{138/134}\text{Ba}$  ranges (–1.08 to –0.22 ‰

and –0.67 to –0.28 ‰, respectively). The Ba contents of metasedimentary wall rocks (125–1238  $\mu\text{g/g}$ ) are significantly higher and more variable than the other samples, but their  $\delta^{138/134}\text{Ba}$  shows a rather restricted range (–0.31 to +0.40 ‰) around a mean of 0.00 ‰, which matches the upper continental crust (UCC,  $0.00 \pm 0.04$  ‰; Nan *et al.*, 2018).

## Discussion

**Controls on Ba isotope variation.** The possible mechanisms driving Ba isotope fractionation in granitoids include chemical alteration, wall rock assimilation, anatexis, and magma differentiation. The first scenario can be excluded as all igneous samples are fresh. Their loss on ignition (LOI) is generally very low ( $\leq 1$  wt. %, Table S-2), the chemical index of alteration (CIA) mostly falls within the range of fresh granitoids, and neither parameter shows any correlation with  $\delta^{138/134}\text{Ba}$  (Fig. S-1). Secondly, because the wall rocks have a limited  $\delta^{138/134}\text{Ba}$  range that is higher than granites, aplites, and most pegmatites, wall rock assimilation could not produce the extremely low  $\delta^{138/134}\text{Ba}$  of most pegmatites. Although some pegmatite samples have similar  $\delta^{138/134}\text{Ba}$  as the wall rocks, they do not show significantly elevated Ba contents except for sample J084317 (higher than all aplites and granites) (Fig. 3a). Therefore, wall rock assimilation cannot explain Ba isotope fractionation between the Jiajika igneous samples.

Some studies suggest that LCT-type pegmatites may result from low degree muscovite dehydration melting of a metasedimentary source containing Li-rich rocks, rather than as products of extreme magma differentiation (Zhao *et al.*, 2022). However, our Ba isotope data do not support this model. According to the dehydration melting reaction  $\text{Muscovite} + \text{Plagioclase} + \text{Quartz} = \text{K-feldspar} + \text{Sillimanite} + \text{melt}$ , K-feldspar should govern the Ba budget of the restite. Because K-feldspar is enriched in light Ba isotopes relative to melts (Deng *et al.*, 2021), the resulting melts should acquire higher  $\delta^{138/134}\text{Ba}$  than the source. In this case, the extremely low  $\delta^{138/134}\text{Ba}$  of most pegmatites implies even lower  $\delta^{138/134}\text{Ba}$  for their source rocks, which is not consistent with the observation of (meta-)sedimentary rocks (Nan *et al.*, 2018). For the pegmatite samples with high  $\delta^{138/134}\text{Ba}$ , their low Rb/Sr does not support muscovite

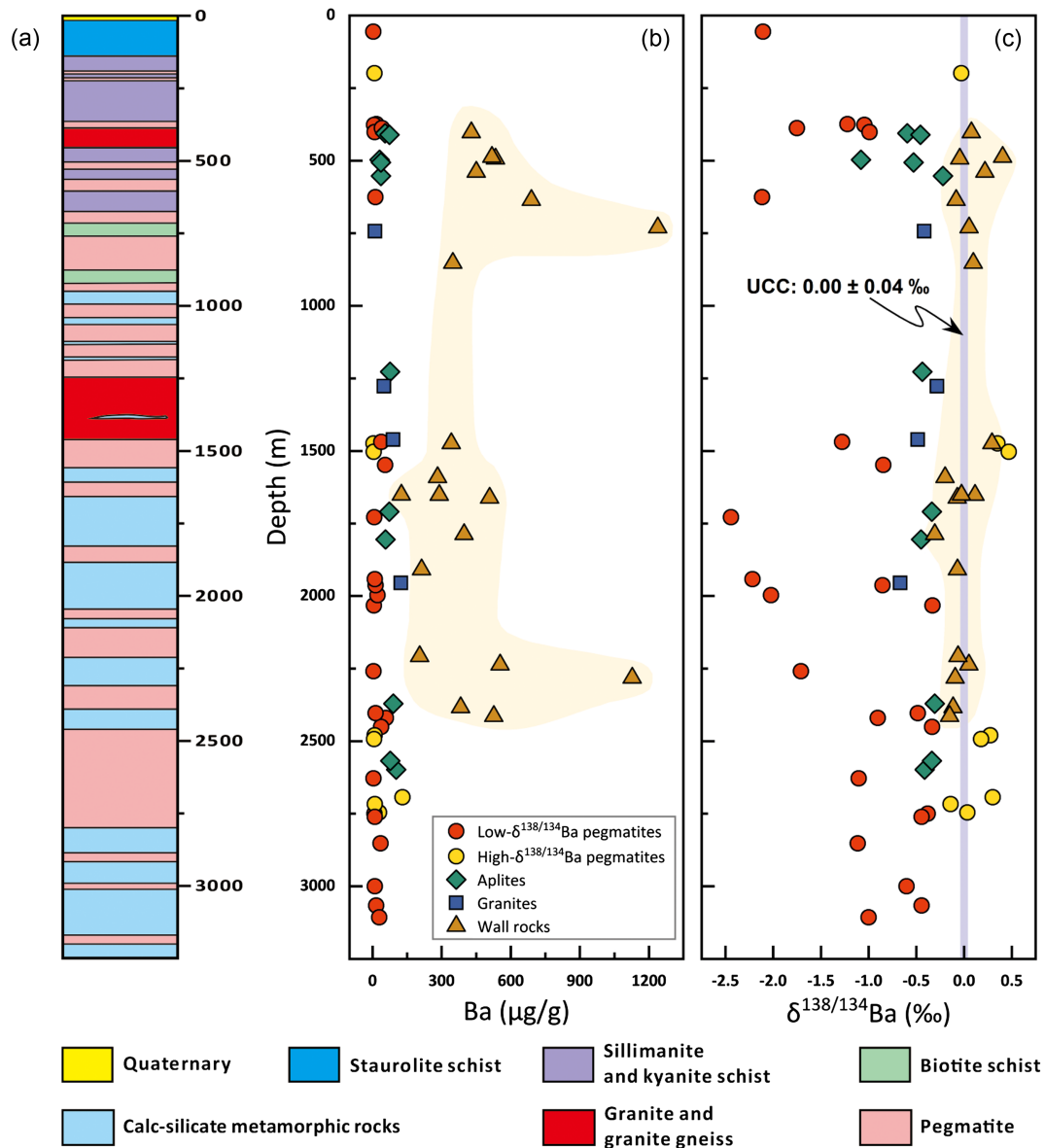


**Figure 2** (a) Schematic cross section of the studied drill hole (modified after Xu *et al.*, 2023). (b) Ba and (c)  $\delta^{138/134}\text{Ba}$  vs. depth. The purple band represents the weighted average  $\delta^{138/134}\text{Ba}$  of the upper continental crust (UCC,  $0.00 \pm 0.04$  ‰; Nan *et al.*, 2018). Error bar is smaller than the symbols.

dehydration melting of a metasedimentary source either (Gao *et al.*, 2017) (Fig. S-2a).

As the vast majority of studies support the Jiajika granite-pegmatite association (Huang *et al.*, 2020; Zhang *et al.*, 2021), the Ba isotope variation among them should be linked to the magma evolution toward pegmatite-forming liquids. Due to the highly evolved nature of the studied granitoids, major element indicators, such as  $\text{SiO}_2$  and  $\text{MgO}$  contents, cannot discern the degree of differentiation (Fig. S-2b,c), while trace element ratios, such as Ba/Rb, can help (Zhang *et al.*, 2021). With the exception of sample J007522, which has abnormally high Ba/Rb likely due to sampling bias, Ba/Rb decreases continuously from granites through aplites to pegmatites (Fig. 3b). This reflects the fractional crystallisation of Ba-rich minerals, which, based on the variation in mineral composition of the borehole samples (Xu *et al.*, 2023), first involves both K-feldspar and mica, and then is dominated by K-feldspar. Because K-feldspar and mica preferentially incorporate light and heavy Ba isotopes, respectively (Deng *et al.*, 2021), such fractional crystallisation can explain the overall consistent  $\delta^{138/134}\text{Ba}$  of

granites and aplites, as well as the elevated  $\delta^{138/134}\text{Ba}$  of some pegmatites (Fig. 3b). However, it cannot account for the significantly lower  $\delta^{138/134}\text{Ba}$  and higher  $\text{K}_2\text{O}$  contents of most pegmatites than those of granites and aplites (Fig. S-2d).

The low  $\delta^{138/134}\text{Ba}$  and high  $\text{K}_2\text{O}$  contents of most pegmatites cannot be explained by crystallisation within pegmatite veins. According to the constitutional zone refining model, light Ba isotopes with higher diffusivity can preferentially feed mineral crystallisation through the boundary layer liquid. Meanwhile, the variation in mineral assemblage of the Jiajika pegmatites indicates that the early crystalline minerals are dominated by Ba- and K-rich microcline that preferentially incorporates light Ba isotopes. Thus,  $\delta^{138/134}\text{Ba}$  of most pegmatites is expected to gradually increase with decreasing Ba and K contents, which is not observed (Figs. 3d, S-2d). Furthermore, although Fe isotope fractionation among these pegmatite samples was suggested to result from fractional crystallisation (Luo *et al.*, 2024), no significant correlation between  $\delta^{138/134}\text{Ba}$  and  $\delta^{56}\text{Fe}$  is seen (Fig. S-2e).

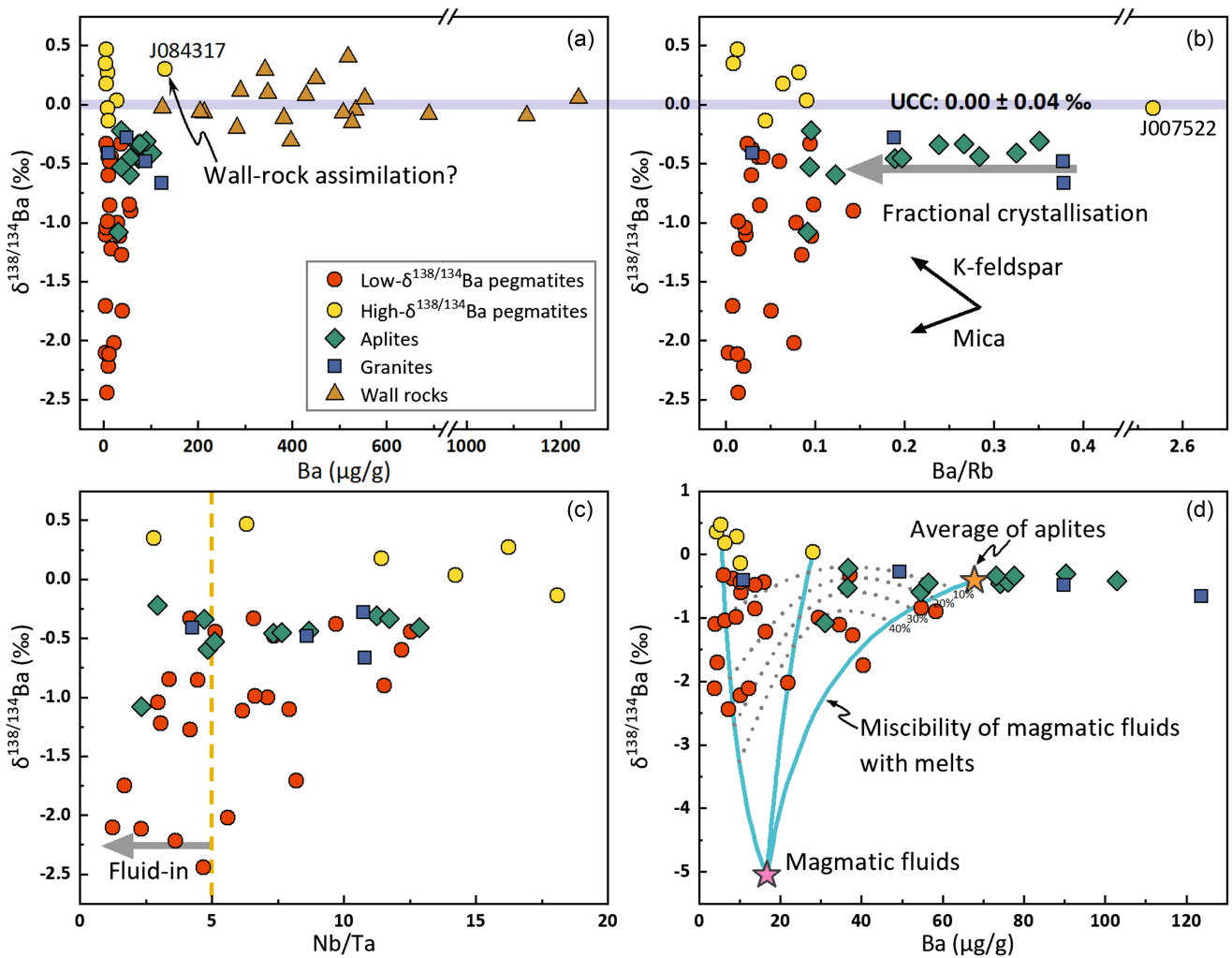


**Figure 3**  $\delta^{138/134}\text{Ba}$  vs. (a) Ba, (b) Ba/Rb, and (c) Nb/Ta. Arrows in (b) indicate evolution of melts during fractional crystallisation of K-feldspar and mica. (d) Simulation of magmatic fluids mixing with highly differentiated melts and comparison with observations. Numbers on the line of mixing denote the fraction of magmatic fluids. The purple band represents the weighted average  $\delta^{138/134}\text{Ba}$  of the UCC. Error bar is smaller than the symbols.

The most likely process responsible for the low  $\delta^{138/134}\text{Ba}$  of pegmatites is modification by magmatic fluids. According to a previous experimental study by Guo *et al.* (2020), the apparent Ba isotope fractionation factor between exsolved fluids and residual melts can be up to  $-4.6$  to  $-5.1$  ‰ under the near solidus cold storage conditions ( $650$ – $600$  °C) of the shallow “mushy” magma reservoirs (Rubin *et al.*, 2017). Considering the generally low Ba contents of most pegmatites ( $<50$   $\mu\text{g/g}$  with an average of  $17.7$   $\mu\text{g/g}$ ), their extremely low  $\delta^{138/134}\text{Ba}$  could well be the result of the incorporation of magmatic fluids into the pegmatite-forming liquids. This interpretation is in line with their tendency towards low Nb/Ta ( $<5$ ) and Zr/Hf ( $<26$ ) (Figs. 3c, S-2f), which are often interpreted as results from magmatic-hydrothermal interaction (Ballouard *et al.*, 2016). The slightly higher Nb/Ta and Zr/Hf of some low- $\delta^{138/134}\text{Ba}$  pegmatites are likely influenced by the crystallisation of accessory minerals, such as columbite-tantalite and zircon, indicating that Ba isotopes might be more sensitive to magmatic fluid activity than these elemental indicators. Consistent with our conclusion, the B and Li isotope compositions (also fluid-mobile elements) of the Jiajika pegmatites have been demonstrated to be significantly modified by magmatic fluids (Zhang *et al.*, 2021; Huan *et al.*, 2023). Metamorphic dehydrated fluids from the wall rocks are enriched in heavy Ba isotopes (Wu *et al.*,

2020), thus cannot provide the light Ba isotope compositions for most pegmatites.

To further decipher the exact mechanism of magmatic fluid participation in pegmatite formation, a model of magmatic fluid mixing with highly differentiated melt is developed in a  $\delta^{138/134}\text{Ba}$ -Ba diagram. Because of continuous decompression and crystallisation, fluid exsolution can occur early in magma evolution and throughout the magma ascent path (Edmonds and Woods, 2018). Thus, when calculating the composition of the magmatic fluid using the Rayleigh fractionation equations, the initial melt is represented by the average of all granites and aplites from various depths. The average of aplite samples and two pegmatites with elevated  $\delta^{138/134}\text{Ba}$  and different Ba/Rb ratios covering the main Ba/Rb range of Jiajika pegmatites are selected to represent highly differentiated melts. The calculations and results are detailed in the Supplementary Information.

As shown in Figure 3d, the variations in Ba elemental and isotope compositions of most pegmatite samples can be explained by the mixing of 10–40 % magmatic fluids with melts of different degrees of evolution. This range of fluid proportions is much wider than that of typical granitic magmas, but it is consistent with the supercritical fluids model of the pegmatite-forming liquids. The studies of melt and fluid inclusions show that

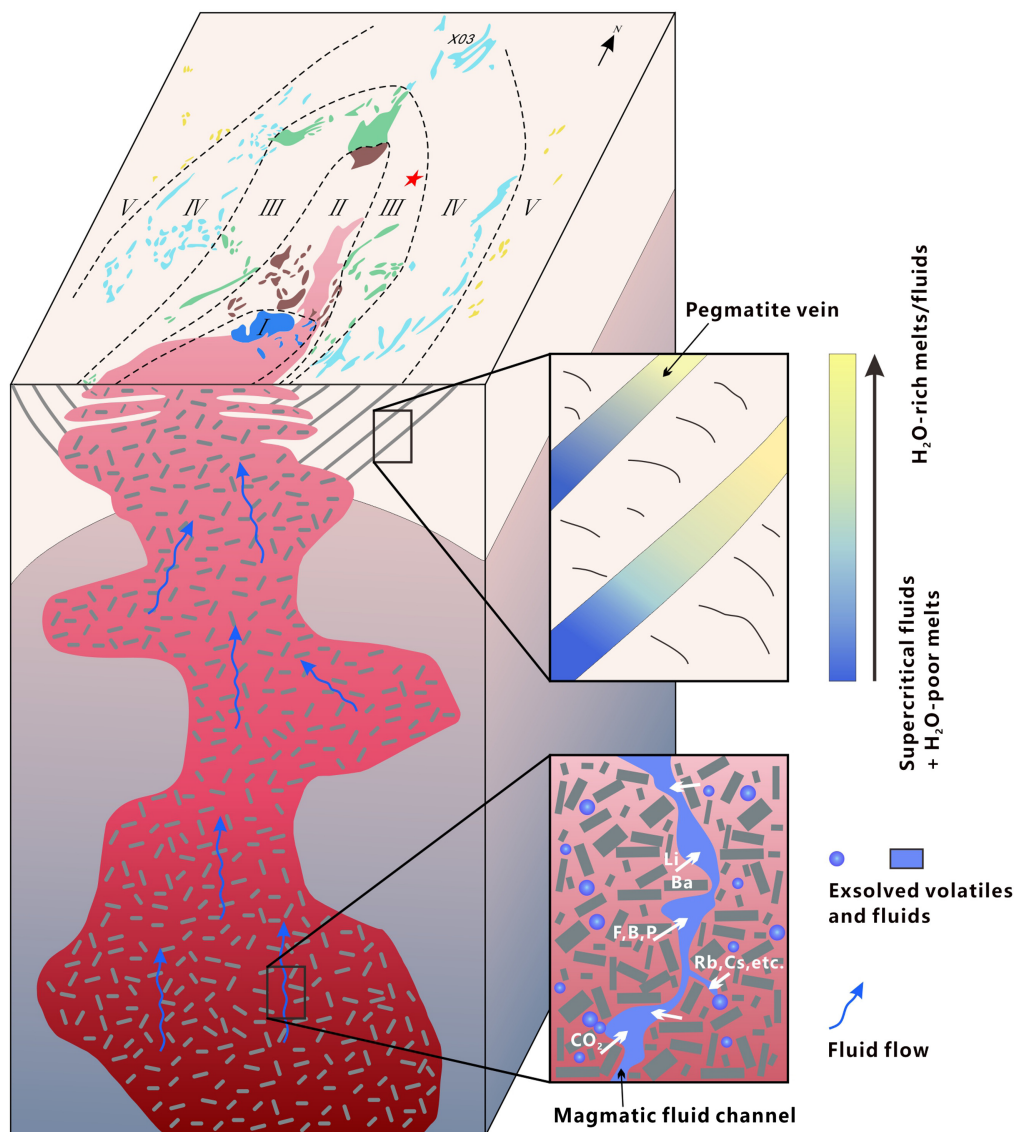


**Figure 4** Schematic model for the role of magmatic fluids in intra-crustal material transport and petrogenesis and metallogenesis of granitic pegmatites.

supercritical fluids have initial water contents ranging from 20 to 33.3 % (Thomas and Davidson, 2016). After intrusion, they separate into conjugated H<sub>2</sub>O-poor melts and H<sub>2</sub>O-rich melts/fluids by melt-melt-fluid immiscibility. The former become the pegmatites with low fluid proportions, while the latter can continue to migrate away from the parental granite due to low viscosities and high mobilities (Troch *et al.*, 2022). Potential supercritical fluid activity in the Jiajika pegmatite field is also supported by previous observations of melt/fluid inclusions. Firstly, representative primary inclusions are commonly enriched in H<sub>2</sub>O, fluxing components, alkaline elements, CO<sub>2</sub>, and carbonates, but depleted in alkaline earth elements (Li and Chou, 2017; J. Deng *et al.*, 2022). These features are similar to those found in other pegmatites showing supercritical fluid activity (Thomas *et al.*, 2019; Wang *et al.*, 2023), and could explain the higher K<sub>2</sub>O contents of most pegmatites compared to granites and aplites. Secondly, the trapping conditions of these inclusions (500–720 °C, 3–5 kbar) are consistent with the critical conditions for the complete miscibility of silicate melts with fluids obtained from experiments with addition of B, F, and Na (600 °C, 4 kbar) (Sowerby and Keppler, 2002). In this case, the multiple magmatic-hydrothermal events experienced by the Jiajika

pegmatites (Xu *et al.*, 2023) could result from multiple injections of supercritical fluids, thereby leading to the lack of systematic variation in their  $\delta^{138/134}\text{Ba}$  with depth. Overall, the Ba isotope signatures of our studied deep pegmatites unequivocally demonstrate that magmatic fluids should overwhelmingly influence the composition and nature of the system from the early stages of pegmatite formation. Barium isotopes can therefore be used in studies of supercritical fluid activity associated with pegmatite systems.

*Implications for Li enrichment in granitic pegmatites.* Despite the importance of granitic pegmatite Li deposits in securing future lithium supply, the mechanism behind Li enrichment, exceeding thousands of times the average continental crust in the formation of such deposits, remains enigmatic. The substantial involvement of magmatic fluids in the petrogenesis of LCT-type pegmatites revealed by our study implies that they should be a key medium in extracting, concentrating, and transporting Li to provide a material source for mineralisation in granitic pegmatites (Fig. 4). The large and super-large pegmatite Li deposits are mainly developed within collisional orogenic belts related to supercontinent assembly

(London, 2018), where thickened crust implies more extensive intra-crustal magmatism. Available geophysical studies indicate the presence of vertically extended (up to 15 km) magma reservoirs beneath a number of LCT-type pegmatites like the Jiajika (Huang *et al.*, 2020). This is consistent with the recent concept of crystal mush-dominated transcrustal magmatic system (Cashman *et al.*, 2017), wherein pegmatites are regarded as the last drops of magmatic distillates at the top (Troch *et al.*, 2022). In such a scenario, hydrothermal fluids stored in shallow magma reservoirs represent the time-integrated products of magmatic differentiation and fluid exsolution operating over a significant vertical extent (Blundy *et al.*, 2021). Because ascending magmatic fluids can be decoupled from residual melts, even the fluid-mobile rare metals and fluxing components enriched in the deep crystal mush can be efficiently extracted and transported to aggregate in shallow magma reservoirs through fluid channels among the crystals (Parmigiani *et al.*, 2016). The elevated contents of fluxing components in shallow magma reservoirs not only effectively reduce the polymerisation of the melts and promote their miscibility with magmatic fluids, but also provide sufficient ligands, thereby enhancing solubility of incompatible rare metals in the resulting supercritical fluids (Thomas and Davidson, 2016). Theoretically, the supercritical fluids can efficiently extract Li and other rare metal elements with enrichment factors of up to  $10^4$  (Thomas *et al.*, 2019). Meanwhile, the accumulated magmatic fluids in shallow magma reservoirs are capable of driving overpressure and causing episodic hydraulic fracturing for supercritical fluids intrusion (Holtzman *et al.*, 2012). Finally, as phase separation occurs to supercritical fluids, Li can be further transported by H<sub>2</sub>O-rich melt/fluid phase to mineralisation away from the parental granite, as shown by the Jiajika and other LCT-type granitic pegmatite fields worldwide (London, 2018; Troch *et al.*, 2022). In short, fluid exsolution within the parental magmatic system provides an additional material source for pegmatite petrogenesis and mineralisation. Liquid immiscibility within pegmatite veins determines the spatial distribution of Li mineralised pegmatites. Therefore, after observing highly differentiated granites with high Li content in the collisional orogenic belts, potential Li-rich pegmatites in wall rocks could occur vertically higher and/or horizontally distant (up to several kilometres), which can be an effective exploration strategy for pegmatite Li deposits.

## Acknowledgements

This work is supported by grants from the Postdoctoral Foundation of China (BH2080000157) and the National Natural Science Foundation of China (GG2080000748).

Editor: Raul O.C. Fonseca

## Additional Information

Supplementary Information accompanies this letter at <https://www.geochemicalperspectivesletters.org/article2426>.



© 2024 The Authors. This work is distributed under the Creative Commons Attribution Non-Commercial No-Derivatives 4.0

License, which permits unrestricted distribution provided the original author and source are credited. The material may not be adapted (remixed, transformed or built upon) or used for commercial purposes without written permission from the author. Additional information is available at <https://www.geochemicalperspectivesletters.org/copyright-and-permissions>.

**Cite this letter as:** Deng, G., Jiang, D., Li, G., Xu, Z., Huang, F. (2024) Barium isotope evidence for a magmatic fluid-dominated petrogenesis of LCT-type pegmatites. *Geochem. Persp. Let.* 31, 14–20. <https://doi.org/10.7185/geochemlet.2426>

## References

- BALLOUARD, C., POUJOL, M., BOULVAIS, P., BRANQUET, Y., TARTESE, R., VIGNERESSE, J.-L. (2016) Nb-Ta fractionation in peraluminous granites: A marker of the magmatic-hydrothermal transition. *Geology* 44, 231–234. <https://doi.org/10.1130/G37475.1>
- BENSON, T.R., COBLE, M.A., RYTUBA, J.J., MAHOOD, G.A. (2017) Lithium enrichment in intracrustal rhyolite magmas leads to Li deposits in caldera basins. *Nature Communications* 8, 270. <https://doi.org/10.1038/s41467-017-00234-y>
- BLUNDY, J., AFINASYEV, A., TATTITCH, B., SPARKS, S., MELNIK, O., UTKIN, I., RUST, A. (2021) The economic potential of metalliferous sub-volcanic brines. *Royal Society Open Science* 8, 202192. <https://doi.org/10.1098/rsos.202192>
- CASHMAN, K.V., SPARKS, R.S.J., BLUNDY, J.D. (2017) Vertically extensive and unstable magmatic systems: A unified view of igneous processes. *Science* 355, eaag3055. <https://doi.org/10.1126/science.aag3055>
- DENG, G., KANG, J., NAN, X., LI, Y., GUO, J., DING, X., HUANG, F. (2021) Barium isotope evidence for crystal-melt separation in granitic magma reservoirs. *Geochimica et Cosmochimica Acta* 292, 115–129. <https://doi.org/10.1016/j.gca.2020.09.027>
- DENG, G., JIANG, D., ZHANG, R., HUANG, J., ZHANG, X., HUANG, F. (2022) Barium isotopes reveal the role of deep magmatic fluids in magmatic-hydrothermal evolution and tin enrichment in granites. *Earth and Planetary Science Letters* 594, 117724. <https://doi.org/10.1016/j.epsl.2022.117724>
- DENG, J., LI, J., ZHANG, D., CHOU, I.-M., YAN, Q., XIONG, X. (2022) Origin of pegmatitic melts from granitic magmas in the formation of the Jiajika lithium deposit in the eastern Tibetan Plateau. *Journal of Asian Earth Sciences* 229, 105147. <https://doi.org/10.1016/j.jseae.2022.105147>
- EDMONDS, M., WOODS, A.W. (2018) Exsolved volatiles in magma reservoirs. *Journal of Volcanology and Geothermal Research* 368, 13–30. <https://doi.org/10.1016/j.jvolgeores.2018.10.018>
- GAO, L.-E., ZENG, L., ASIMOW, P.D. (2017) Contrasting geochemical signatures of fluid-absent versus fluid-fluxed melting of muscovite in metasedimentary sources: The Himalayan leucogranites. *Geology* 45, 39–42. <https://doi.org/10.1130/G38336.1>
- GUO, H., LI, W.-Y., NAN, X., HUANG, F. (2020) Experimental evidence for light Ba isotopes favouring aqueous fluids over silicate melts. *Geochemical Perspectives Letters* 16, 6–11. <http://dx.doi.org/10.7185/geochemlet.2036>
- HOLTZMAN, R., SZULCZEWSKI, M.L., JUANES, R. (2012) Capillary Fracturing in Granular Media. *Physical Review Letters* 108, 264504. <https://link.aps.org/doi/10.1103/PhysRevLett.108.264504>
- HUAN, C., WEI, H.-Z., ZHU, W.-B., PALMER, M.R., LIN, H.-F., ZHENG, B.-H., CAI, Y., ZUO, D.-S., WANG, J.-L., XU, Z.-Q. (2023) Boron isotopes in tourmaline from drill core of the Jiajika granitic pegmatite type lithium deposit: Insights for granitic magma evolution and lithium enrichment. *Ore Geology Reviews* 163, 105742. <https://doi.org/10.1016/j.oregeorev.2023.105742>
- HUANG, F., BAI, R., DENG, G., LIU, X., LI, X. (2021) Barium isotope evidence for the role of magmatic fluids in the origin of Himalayan leucogranites. *Science Bulletin* 66, 2329–2336. <https://doi.org/10.1016/j.scib.2021.07.020>
- HUANG, T., FU, X., GE, L., ZOU, F., HAO, X., YANG, R., XIAO, R., FAN, J. (2020) The genesis of giant lithium pegmatite veins in Jiajika, Sichuan, China: Insights from geophysical, geochemical as well as structural geology approach. *Ore Geology Reviews* 124, 103557. <https://doi.org/10.1016/j.oregeorev.2020.103557>
- LI, J., CHOU, I.-M. (2017) Homogenization Experiments of Crystal-Rich Inclusions in Spodumene from Jiajika Lithium Deposit, China, under Elevated External Pressures in a Hydrothermal Diamond-Anvil Cell. *Geofluids* 2017, 9252913. <https://doi.org/10.1155/2017/9252913>
- LONDON, D. (2014) A petrologic assessment of internal zonation in granitic pegmatites. *Lithos* 184–187, 74–104. <https://doi.org/10.1016/j.lithos.2013.10.025>
- LONDON, D. (2018) Ore-forming processes within granitic pegmatites. *Ore Geology Reviews* 101, 349–383. <https://doi.org/10.1016/j.oregeorev.2018.04.020>
- LUO, X.-L., LI, W., DU, D.-H., AN, S., ZHENG, B., ZHU, W., XU, Z. (2024) Iron isotope systematics of the Jiajika granite-pegmatite lithium deposit, Sichuan, China. *Ore Geology Reviews* 165, 105903. <https://doi.org/10.1016/j.oregeorev.2024.105903>

- NAN, X.-Y., YU, H.-M., RUDNICK, R.L., GASCHNIG, R.M., XU, J., LI, W.-Y., ZHANG, Q., JIN, Z.-D., LI, X.-H., HUANG, F. (2018) Barium isotopic composition of the upper continental crust. *Geochimica et Cosmochimica Acta* 233, 33–49. <https://doi.org/10.1016/j.gca.2018.05.004>
- PARMIGIANI, A., FAROUGH, S., HUBER, C., BACHMANN, O., SU, Y. (2016) Bubble accumulation and its role in the evolution of magma reservoirs in the upper crust. *Nature* 532, 492–495. <https://doi.org/10.1038/nature17401>
- RUBIN, A.E., COOPER, K.M., TILL, C.B., KENT, A.J.R., COSTA, F., BOSE, M., GRAVLEY, D., DEERING, C., COLE, J. (2017) Rapid cooling and cold storage in a silicic magma reservoir recorded in individual crystals. *Science* 356, 1154–1156. <https://doi.org/10.1126/science.aam8720>
- SOWERBY, J.R., KEPPLER, H. (2002) The effect of fluorine, boron and excess sodium on the critical curve in the albite–H<sub>2</sub>O system. *Contributions to Mineralogy and Petrology* 143, 32–37. <https://doi.org/10.1007/s00410-001-0334-5>
- THOMAS, R., DAVIDSON, P. (2016) Revisiting complete miscibility between silicate melts and hydrous fluids, and the extreme enrichment of some elements in the supercritical state — Consequences for the formation of pegmatites and ore deposits. *Ore Geology Reviews* 72, 1088–1101. <https://doi.org/10.1016/j.oregeorev.2015.10.004>
- THOMAS, R., DAVIDSON, P., APPEL, K. (2019) The enhanced element enrichment in the supercritical states of granite–pegmatite systems. *Acta Geochimica* 38, 335–349. <https://doi.org/10.1007/s11631-019-00319-z>
- TROCH, J., HUBER, C., BACHMANN, O. (2022) The physical and chemical evolution of magmatic fluids in near-solidus silicic magma reservoirs: Implications for the formation of pegmatites. *American Mineralogist* 107, 190–205. <https://doi.org/10.2138/am-2021-7915>
- WANG, G.-G., ZHENG, F.-B., NI, P., WU, Y.-W., QI, W.-X., LI, Z.-A. (2023) Fluid properties and ore-forming process of the giant Jiajika pegmatite Li deposit, western China. *Ore Geology Reviews* 160, 105613. <https://doi.org/10.1016/j.oregeorev.2023.105613>
- WU, F., TURNER, S., SCHAEFER, B.F. (2020) Mélange versus fluid and melt enrichment of subarc mantle: A novel test using barium isotopes in the Tonga–Kermadec arc. *Geology* 48, 1053–1057. <https://doi.org/10.1130/G47549.1>
- XU, Z., ZHENG, B., ZHU, W., CHEN, Y., LI, G., GAO, J., CHE, X., ZHANG, R., WEI, H., LI, W., WANG, G., WEI, G., YAN, H. (2023) Geologic scenario from granitic sheet to Li-rich pegmatite uncovered by Scientific Drilling at the Jiajika lithium deposit in eastern Tibetan Plateau. *Ore Geology Reviews* 161, 105636. <https://doi.org/10.1016/j.oregeorev.2023.105636>
- ZHANG, H., TIAN, S., WANG, D., LI, X., LIU, T., ZHANG, Y., FU, X., HAO, X., HOU, K., ZHAO, Y., QIN, Y. (2021) Lithium isotope behavior during magmatic differentiation and fluid exsolution in the Jiajika granite–pegmatite deposit, Sichuan, China. *Ore Geology Reviews* 134, 104139. <https://doi.org/10.1016/j.oregeorev.2021.104139>
- ZHAO, H., CHEN, B., HUANG, C., BAO, C., YANG, Q., CAO, R. (2022) Geochemical and Sr–Nd–Li isotopic constraints on the genesis of the Jiajika Li-rich pegmatites, eastern Tibetan Plateau: implications for Li mineralization. *Contributions to Mineralogy and Petrology* 177, 4. <https://doi.org/10.1007/s00410-021-01869-3>

# Barium isotope evidence for a magmatic fluid-dominated petrogenesis of LCT-type pegmatites

G. Deng, D. Jiang, G. Li, Z. Xu, F. Huang

## Supplementary Information

The Supplementary Information includes:

- Geological Background and Samples
- Analytical Method
- Simulation of Magmatic Fluid Mixing with Highly Differentiated Melts
- Figures S-1 and S-2
- Tables S-1 to S-3
- Supplementary Information References

## Geological Background and Samples

The Sonpan-Ganze orogenic belt (SGOB) is located in the northeastern margin of the Tibetan Plateau and stretches east-west for more than 2800 km (Xu *et al.*, 2020). The SGOB formed during the Middle to Late Triassic closure of the Paleo-Tethys Ocean, and overall exhibits a distinctive triangular shape (Yin and Harrison, 2000). It is bounded by the Kunlun-Qaidam Terrane to the north, the Qiangtang Terrane to the south, and the Yangtze Block to the east (Xu *et al.*, 2020). A large number of 228–195 Ma syn- and post-orogenic granites are widely developed within the SGOB, and the Sr-Nd isotope compositions indicate that the magma should be mainly derived from partial melting of the basement rocks and cover sediments of the orogenic belt in the source, with a small contribution from mantle derived material (Roger *et al.*, 2004; Zhang *et al.*, 2006). Recently, several large to super-large pegmatite Li-Be deposits have been discovered in the eastern part of the SGOB, constituting an important mineralization zone of rare metals (Huang *et al.*, 2020; Zheng *et al.*, 2020). These pegmatite Li-Be deposits are hosted within gneiss domes such as Jiajika, Danba,

Markam, Keeryin and Zawulong, which are characterized by Triassic granite cores enveloped by Triassic metamorphic rocks (Xu *et al.*, 2020).

The Jiajika gneiss dome has a core of Majingzi two-mica granite and a set of Triassic metasedimentary rocks in the mantle. The Majingzi two-mica granite belongs to peraluminous S-type granite, with an exposed area of about 5.5 km<sup>2</sup> (Huang *et al.*, 2020). The metasedimentary rocks are the result of high-temperature, middle-low pressure metamorphism of the Xikang Group strata. They are well-zoned surrounding the Majingzi granite, with sillimanite, staurolite-andalusite, garnet-biotite and sericite-chlorite zones from the interior to the margins (Xu *et al.*, 2020). More than 500 granitic pegmatite veins have been found in the two-mica granite and metasedimentary rocks covering an area of ~60 km<sup>2</sup>. These pegmatites can be divided into five zones surrounding the two-mica granite, which are, in order from the pluton outward, microcline pegmatite (I), microcline-albite pegmatite (II), albite pegmatite (III), albite-spodumene pegmatite (IV) and albite-lepidolite pegmatite (V). However, these pegmatite veins generally lack obvious internal zonation (Huang *et al.*, 2020), with only a few showing simple zonation (wall and inner zone) (Zhao *et al.*, 2021). They typically show sharp contact with wall-rocks (Zhang *et al.*, 2021). Previous studies have shown that the Majingzi granite and the pegmatites were mainly emplaced at ~223–208 Ma and ~216.3–215.5 Ma, respectively (Huang *et al.*, 2020). Li mineralization is mainly developed within zones IV and V, as well as some veins in zone III, with a total estimated Li<sub>2</sub>O reserves of up to 3.0 Mt, ranking the first in Asia (Huang *et al.*, 2020). Li mineralized pegmatites typically comprise mainly albite, microcline, spodumene, quartz, muscovite, calcite, and chlorite, with minor minerals such as apatite, beryl, zircon, cookeite, cassiterite, and columbite-tantalite (Wang *et al.*, 2023). In addition, Be mineralization can be observed in some pegmatite veins of zones I and II (Huang *et al.*, 2020).

The borehole samples used in this study are from the Jiajika Scientific Drilling (JSD-1) project (Xu *et al.*, 2023). The drill hole was located ~1 km away to the northeast of the Majingzi granite (101°16'39.34" E, 30°17'16.31" N), at an altitude of 4425 m, and was drilled to a final depth of 3211.21 m. The JSD-1 core consists of 35 % metasediments, 14 % granite-aplites and 51 % pegmatites. The metasedimentary rocks can be divided into two units. The upper unit (<900 m in depth) is mainly schists, while the lower unit contains metamorphic calc-silicate rocks and biotite schists. Two granite sheets are identified at the depths of 418–440 m and 1245–1455 m, respectively. The greyish-white two-mica granites typically consist of quartz (35–40 %), microcline (20–30 %), albite (20–30 %), minor muscovite (1–5 %), and biotite (1–5 %) (Luo *et al.*, 2024). Corresponding to the classification of metasedimentary rocks, aplites can also be divided into two categories. Layered aplites mostly occur at depths less than 900 m and consist of dark and light oscillating bands, with plagioclase and quartz in the light layers and additional tourmaline and garnet in the dark layers. Whereas, below 900 m, the aplites generally lack apparent layering (Xu *et al.*, 2023). The mineral composition of pegmatites varies significantly with depth. Spodumene, the only Li-rich mineral, is present only in albite-spodumene pegmatites at depths less than 100 m. This leads to a dramatic increase in the whole-rock Li contents of pegmatites (from ~40 µg/g to 6000 µg/g) (Xu *et al.*, 2023). The spodumene-barren pegmatites are widely distributed below 100 m, with the main mineral compositions of microcline, albite, quartz, muscovite, biotite, tourmaline, beryl, and garnet. A gradual decrease in microcline and biotite with a gradual increase in albite and tourmaline are observed in the pegmatites

from bottom to top along JSD-1 core. In addition to Li, the contents of other rare metal elements in the pegmatites also increase markedly from different depths (*e.g.*, Be < 800 m, Nb, Ta < 1700 m) (Jin *et al.*, 2023). Monazite and columbite-group minerals U-Pb dating results showed that most pegmatites in JSD-1 core have a similar age range (213–205 Ma) to the granites (208–205 Ma) (Zhou *et al.*, 2023; Zhu *et al.*, 2023). Some younger albite pegmatites (193–190 Ma) with Nb-Ta mineralization were additionally observed at depths of 3170–3211 m, suggesting at least two episodes of magmatic-hydrothermal events (Jin *et al.*, 2023; Zhou *et al.*, 2023; Zhu *et al.*, 2023).

## Analytical Method

In this study, 32 granitic pegmatites, 11 granitic aplites, 4 granites and 19 metasedimentary wall-rocks were collected from different depths of the JSD-1 core. For pegmatites, in order to avoid possible sampling bias due to their coarse crystals, each sample contained as far as possible a representative mineral assemblage of the sampled pegmatites.

Barium isotopes were analysed at the CAS Key Laboratory of Crust-Mantle Materials and Environments in the University of Science and Technology of China. Nan *et al.* (2015, 2018) described in detail the sample dissolution, chemical purification, and instrumental measurement, and the brief description is as follows. Sample powders containing ~2 µg Ba were dissolved with a 3:1 (v/v) mixture of HF–HNO<sub>3</sub> in 7 mL Teflon PFA screw-top beakers (Savillex). After drying, the samples were treated with aqua regia and concentrated HCl to remove fluorides. Barium was purified from the matrix using cation exchange resin (AG50W-X12, 200–400 mesh, Bio-Rad, USA). Ba was collected with 3 mol/L HNO<sub>3</sub> after eluting the matrix elements using 3 mol/L HCl. The purified samples were dried and diluted with 2 % HNO<sub>3</sub> for measurement. The yields of the purification process were >99 % and the total procedural blank was <5 ng. Ba isotope compositions were measured on a Neptune-Plus multi-collector inductively coupled plasma mass spectrometer (MC-ICP-MS, Thermo-Fisher Scientific). Instrumental mass discrimination was corrected using the <sup>135</sup>Ba–<sup>136</sup>Ba double-spike method. Sample solutions were introduced with an Aridus II desolvator (CETAC Technologies, USA) to reduce the formation of polyatomic ions (*e.g.*, BaO<sup>+</sup>) and increase sensitivity (~30 V/100 ng/g for <sup>138</sup>Ba). Normal Ni sampler and Ni X skimmer cones and the low-resolution mode were adopted for measurement, with <sup>134</sup>Ba, <sup>135</sup>Ba, <sup>136</sup>Ba, <sup>137</sup>Ba and <sup>138</sup>Ba collected simultaneously by the L2, L1, C, H1 and H2 Faraday cups, respectively. <sup>131</sup>Xe and <sup>140</sup>Ce were also collected by L4 and H3 Faraday cups, respectively, to correct the effects of isobaric interferences. The background signals for <sup>138</sup>Ba (<0.02 V) were negligible relative to the sample signals.

## Simulation of Magmatic Fluid Mixing with Highly Differentiated Melts

To further decipher the exact mechanism of magmatic fluid participation in pegmatite formation, a model of magmatic fluid mixing with highly differentiated melt is developed in δ<sup>138/134</sup>Ba–Ba diagram. The magmatic fluids exsolved from

the underlying magma reservoirs, and their Ba contents and Ba isotope compositions can be calculated by respective Rayleigh fractionation equations:

$$C_{\text{fluid}} = C_0 \cdot [1 - (1 - F)^D] / F \quad (\text{S-1})$$

$$\delta^{138/134}\text{Ba}_{\text{fluid}} = (\delta^{138/134}\text{Ba}_0 + 1000)(f^\alpha - 1) / (f - 1) - 1000 \quad (\text{S-2})$$

where  $C_0$  and  $\delta^{138/134}\text{Ba}_0$  are the Ba content and Ba isotope composition of the initial melt, respectively, represented by the average of granite and aplite samples (except for sample J018509 with obviously lower  $\delta^{138/134}\text{Ba}$ ), and  $F$  and  $f$  are the fractions of fluid exsolution and Ba remaining in the melt, respectively, and  $D$  and  $\alpha$  are the bulk partition coefficient and the equilibrium fractionation factor between fluid and melt, respectively. The  $D$  and  $\alpha$  are calculated based on the regression equations involving temperature, fluid salinity, and melt ASI, obtained experimentally by Guo *et al.* (2020). Temperatures of 650 °C and 600 °C are used because of the long-term cold storage of the shallow magmatic system at near-solidus or even lower temperatures (Rubin *et al.*, 2017; Szymanowski *et al.*, 2017). The fluid salinity and melt ASI are obtained from fluid inclusions and the average of granite and aplite samples, respectively (Table S-2). Since the fluid exsolving proportion in silicate melts is typically less than 10 % (Edmonds and Woods, 2018), the calculated results with a proportion of 10 % (i.e.  $F = 0.1$ ) are used as the composition ranges of the magmatic fluids. The results show that temperature variation (650 °C and 600 °C) has small influences on the Ba content and  $\delta^{138/134}\text{Ba}$  of the magmatic fluids (Table S-2), so the averages of results corresponding to the two temperatures are used in the subsequent mixing simulation.

As the K-feldspar-controlled crystallization would lead to an elevated  $\delta^{138/134}\text{Ba}$  in the residual melts, the average of aplite samples (except for sample J018509 with obviously lower  $\delta^{138/134}\text{Ba}$ ) and two pegmatites with elevated  $\delta^{138/134}\text{Ba}$  and different Ba/Rb ratios covering the main Ba/Rb range of Jiajika pegmatites are selected to represent highly differentiated melts (i.e.  $C_{\text{melt}}$  and  $\delta^{138/134}\text{Ba}_{\text{melt}}$ ). Then the Ba contents and  $\delta^{138/134}\text{Ba}$  of the mixtures can be described by the respective following mass balance equations:

$$C_{\text{mix}} = f_{\text{fluid}} \cdot C_{\text{fluid}} + (1 - f_{\text{fluid}}) \cdot C_{\text{melt}} \quad (\text{S-3})$$

$$\delta^{138/134}\text{Ba}_{\text{mix}} \cdot C_{\text{mix}} = \delta^{138/134}\text{Ba}_{\text{fluid}} \cdot f_{\text{fluid}} \cdot C_{\text{fluid}} + \delta^{138/134}\text{Ba}_{\text{melt}} \cdot (1 - f_{\text{fluid}}) \cdot C_{\text{melt}} \quad (\text{S-4})$$

where  $f_{\text{fluid}}$  is the fraction of the mixed magmatic fluids. The calculated results are reported in Table S-3 and are shown in Figure 3d.

## Supplementary Figures

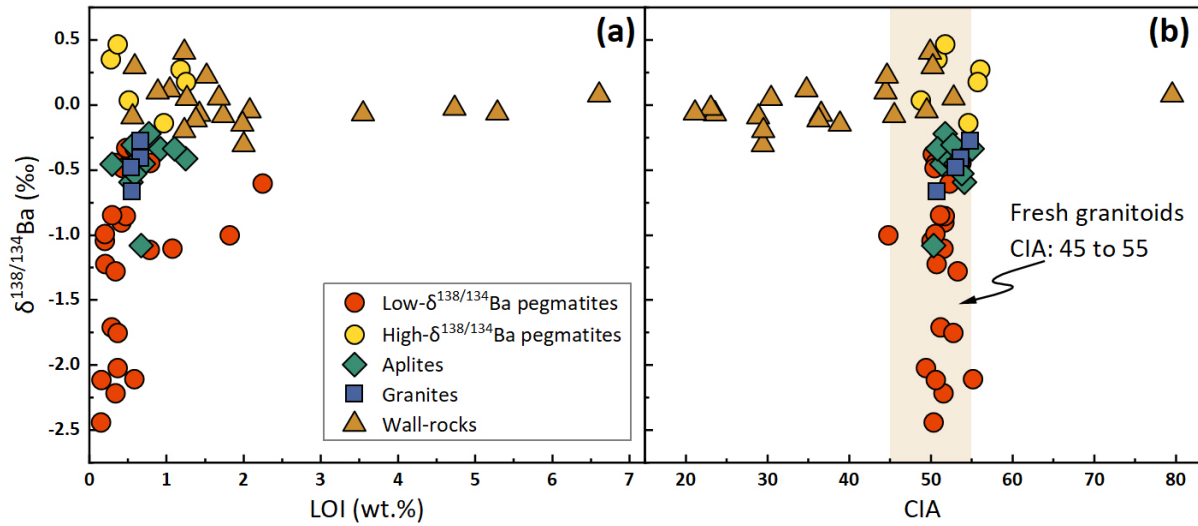


**Figure S-1** (a) LOI and (b) CIA vs.  $\delta^{138/134}\text{Ba}$  for samples from the Jiajika scientific drilling project. Error bar is smaller than the symbols. The CIA range of fresh granitoids comes from Nesbitt and Young (1982).

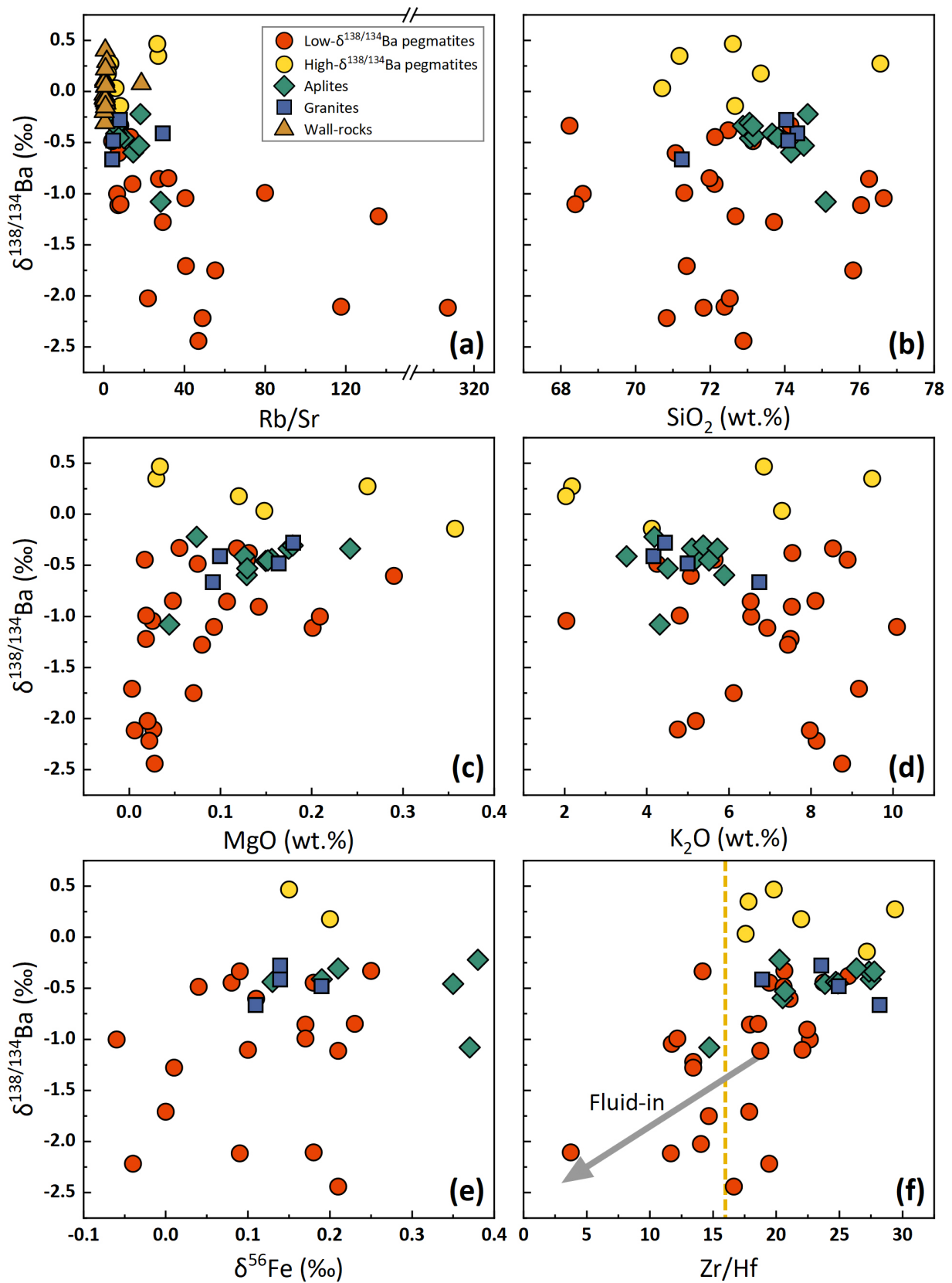


**Figure S-2** (a) Rb/Sr, (b) SiO<sub>2</sub>, (c) MgO, (d) K<sub>2</sub>O, (e) δ<sup>56</sup>Fe and (f) Zr/Hf vs. δ<sup>138/134</sup>Ba for samples from the Jiajika scientific drilling project. Error bar is smaller than the symbols.

## Supplementary Tables

**Table S-1** Location and grade data for representative Li deposits worldwide.

**Table S-2** Information and Ba isotope compositions of samples from the Jiajika scientific drilling project.

**Table S-3** Procedures and results of the quantitative modelling.

Tables S-1 to S-3 are available for download (.xlsx) from the online version of this article at <http://doi.org/10.7185/geochemlet.2426>.

## Supplementary Information References

- An, Y.-J., Li, X., Zhang, Z.-F. (2020) Barium Isotopic Compositions in Thirty-Four Geological Reference Materials Analysed by MC-ICP-MS. *Geostandards and Geoanalytical Research* 44, 183–199. <https://doi.org/10.1111/ggr.12299>
- Barnes, E.M., Weis, D., Groat, L.A. (2012) Significant Li isotope fractionation in geochemically evolved rare element-bearing pegmatites from the Little Nahanni Pegmatite Group, NWT, Canada. *Lithos* 132–133, 21–36. <https://doi.org/10.1016/j.lithos.2011.11.014>
- Bowell, R.J., Lagos, L., de los Hoyos, C.R., Declercq, J. (2020) Classification and Characteristics of Natural Lithium Resources. *Elements* 16, 259–264. <https://doi.org/10.2138/gselements.16.4.259>
- Camacho, A., Baadsgaard, H., Davis, D.W., Černý, P. (2012) RADIOGENIC ISOTOPE SYSTEMATICS OF THE TANCO AND SILVERLEAF GRANITIC PEGMATITES, WINNIPEG RIVER PEGMATITE DISTRICT, MANITOBA. *The Canadian Mineralogist* 50, 1775–1792. <https://doi.org/10.3749/canmin.50.6.1775>
- Deng, G., Kang, J., Nan, X., Li, Y., Guo, J., Ding, X., Huang, F. (2021) Barium isotope evidence for crystal-melt separation in granitic magma reservoirs. *Geochimica et Cosmochimica Acta* 292, 115–129. <https://doi.org/10.1016/j.gca.2020.09.027>
- Deng, G., Jiang, D., Zhang, R., Huang, J., Zhang, X., Huang, F. (2022) Barium isotopes reveal the role of deep magmatic fluids in magmatic-hydrothermal evolution and tin enrichment in granites. *Earth and Planetary Science Letters* 594, 117724. <https://doi.org/10.1016/j.epsl.2022.117724>
- Edmonds, M., Woods, A.W. (2018) Exsolved volatiles in magma reservoirs. *Journal of Volcanology and Geothermal Research* 368, 13–30. <https://doi.org/10.1016/j.jvolgeores.2018.10.018>
- Gong, Y., Zeng, Z., Zhou, C., Nan, X., Yu, H., Lu, Y., Li, W., Gou, W., Cheng, W., Huang, F. (2019) Barium isotopic fractionation in latosol developed from strongly weathered basalt. *Science of The Total Environment* 687, 1295–1304. <https://doi.org/10.1016/j.scitotenv.2019.05.427>
- Gou, L.-F., Deng, L. (2019) Determination of Barium Isotopic Ratios in River Water on the Multiple Collector Inductively Coupled Plasma Mass Spectrometer. *Analytical Sciences* 35, 521–527. <https://doi.org/10.2116/analsci.18P329>
- Guo, H., Li, W.-Y., Nan, X., Huang, F. (2020) Experimental evidence for light Ba isotopes favouring aqueous fluids over silicate melts. *Geochemical Perspectives Letters* 16, 6–11. <http://dx.doi.org/10.7185/geochemlet.2036>

- Hu, X.-j., Li, H. (2021) Research progress and prospect of granitic pegmatite-type lithium deposits. *The Chinese Journal of Nonferrous Metals* 31, 3468–3488. <https://doi.org/10.11817/j.ysxb.1004.0609.2021-42169>
- Huang, T., Fu, X., Ge, L., Zou, F., Hao, X., Yang, R., Xiao, R., Fan, J. (2020) The genesis of giant lithium pegmatite veins in Jiajika, Sichuan, China: Insights from geophysical, geochemical as well as structural geology approach. *Ore Geology Reviews* 124, 103557. <https://doi.org/10.1016/j.oregeorev.2020.103557>
- Jin, W., Che, X., Wang, R., Xu, Z., Hu, H., Zhang, R., Li, G., Zheng, B. (2023) The deep rare metal metallogenic characteristics of the Jiajika lithium polymetallic deposit in Sichuan Province, China: Revealed by the Jiajika Scientific Drilling. *Ore Geology Reviews* 160, 105579. <https://doi.org/10.1016/j.oregeorev.2023.105579>
- Kesler, S.E., Gruber, P.W., Medina, P.A., Keoleian, G.A., Everson, M.P., Wallington, T.J. (2012) Global lithium resources: Relative importance of pegmatite, brine and other deposits. *Ore Geology Reviews* 48, 55–69. <https://doi.org/10.1016/j.oregeorev.2012.05.006>
- Kinny, P. (2000) U–Pb dating of rare-metal (Sn–Ta–Li) mineralized pegmatites in Western Australia by SIMS analysis of tin and tantalum-bearing ore minerals. *New Frontiers in Isotope Geoscience Conference*, University of Melbourne, Victoria, February 2000, 113–116.
- Krogstad, E.J., Walker, R.J. (1994) High closure temperatures of the U–Pb system in large apatites from the Tin Mountain pegmatite, Black Hills, South Dakota, USA. *Geochimica et Cosmochimica Acta* 58, 3845–3853. [https://doi.org/10.1016/0016-7037\(94\)90367-0](https://doi.org/10.1016/0016-7037(94)90367-0)
- Lasmanis, R. (1978) Lithium resources in the Yellowknife area, Northwest Territories, Canada. *Energy* 3, 399–407. [https://doi.org/10.1016/0360-5442\(78\)90037-3](https://doi.org/10.1016/0360-5442(78)90037-3)
- Liu, L., Wang, D., Liu, X., Li, J., Dai, H., Yan, W. (2017) The main types, distribution features and present situation of exploration and development for domestic and foreign lithium mine. *Geology in China* 44, 263–278. <https://doi.org/10.12029/gc20170204>
- Luo, X.-L., Li, W., Du, D.-H., An, S., Zheng, B., Zhu, W., Xu, Z. (2024) Iron isotope systematics of the Jiajika granite-pegmatite lithium deposit, Sichuan, China. *Ore Geology Reviews* 165, 105903. <https://doi.org/10.1016/j.oregeorev.2024.105903>
- Melcher, F., Graupner, T., Gäbler, H.-E., Sitnikova, M., Henjes-Kunst, F., Oberthür, T., Gerdes, A., Dewaele, S. (2015) Tantalum–(niobium–tin) mineralisation in African pegmatites and rare metal granites: Constraints from Ta–Nb oxide mineralogy, geochemistry and U–Pb geochronology. *Ore Geology Reviews* 64, 667–719. <https://doi.org/10.1016/j.oregeorev.2013.09.003>
- Nan, X., Wu, F., Zhang, Z., Hou, Z., Huang, F., Yu, H. (2015) High-precision barium isotope measurements by MC-ICP-MS. *Journal of Analytical Atomic Spectrometry* 30, 2307–2315. <https://doi.org/10.1039/C5JA00166H>
- Nan, X.-Y., Yu, H.-M., Rudnick, R.L., Gaschnig, R.M., Xu, J., Li, W.-Y., Zhang, Q., Jin, Z.-D., Li, X.-H., Huang, F. (2018) Barium isotopic composition of the upper continental crust. *Geochimica et Cosmochimica Acta* 233, 33–49. <https://doi.org/10.1016/j.gca.2018.05.004>
- Nesbitt, H.W., Young, G.M. (1982) Early Proterozoic climates and plate motions inferred from major element chemistry of lutites. *Nature* 299, 715–717. <https://doi.org/10.1038/299715a0>
- Partington, G.A., McNaughton, N.J., Williams, I.S. (1995) A review of the geology, mineralization, and geochronology of the Greenbushes Pegmatite, Western Australia. *Economic Geology* 90, 616–635. <https://doi.org/10.2113/gsecongeo.90.3.616>
- Roger, F., Malavieille, J., Leloup, Ph.H., Calassou, S., Xu, Z. (2004) Timing of granite emplacement and cooling in the Songpan–Garzê Fold Belt (eastern Tibetan Plateau) with tectonic implications. *Journal of Asian Earth Sciences* 22, 465–481. [https://doi.org/10.1016/S1367-9120\(03\)00089-0](https://doi.org/10.1016/S1367-9120(03)00089-0)

- Rubin, A.E., Cooper, K.M., Till, C.B., Kent, A.J.R., Costa, F., Bose, M., Gravley, D., Deering, C., Cole, J. (2017) Rapid cooling and cold storage in a silicic magma reservoir recorded in individual crystals. *Science* 356, 1154–1156. <https://doi.org/10.1126/science.aam8720>
- Simmons, W.B., Falster, A.U., Freeman, G. (2020) The Plumbago North pegmatite, Maine, USA: a new potential lithium resource. *Mineralium Deposita* 55, 1505–1510. <https://doi.org/10.1007/s00126-020-00956-y>
- Szymanowski, D., Wotzlaw, J.-F., Ellis, B.S., Bachmann, O., Guillong, M., von Quadt, A. (2017) Protracted near-solidus storage and pre-eruptive rejuvenation of large magma reservoirs. *Nature Geoscience* 10, 777–782. <https://doi.org/10.1038/ngeo3020>
- van Zuilen, K., Müller, T., Nägler, T.F., Dietzel, M., Küsters, T. (2016) Experimental determination of barium isotope fractionation during diffusion and adsorption processes at low temperatures. *Geochimica et Cosmochimica Acta* 186, 226–241. <http://dx.doi.org/10.1016/j.gca.2016.04.049>
- Wang, G.-G., Zheng, F.-B., Ni, P., Wu, Y.-W., Qi, W.-X., Li, Z.-A. (2023) Fluid properties and ore-forming process of the giant Jiajika pegmatite Li deposit, western China. *Ore Geology Reviews* 160, 105613. <https://doi.org/10.1016/j.oregeorev.2023.105613>
- Xu, Z., Fu, X., Wang, R., Li, G., Zheng, Y., Zhao, Z., Lian, D. (2020) Generation of lithium-bearing pegmatite deposits within the Songpan-Ganze orogenic belt, East Tibet. *Lithos* 354–355, 105281. <https://doi.org/10.1016/j.lithos.2019.105281>
- Xu, Z., Zheng, B., Zhu, W., Chen, Y., Li, G., Gao, J., Che, X., Zhang, R., Wei, H., Li, W., Wang, G., Wei, G., Yan, H. (2023) Geologic Scenario from Granitic sheet to Li-rich Pegmatite Uncovered by Scientific Drilling at the Jiajika Lithium Deposit in Eastern Tibetan Plateau. *Ore Geology Reviews* 161, 105636. <https://doi.org/10.1016/j.oregeorev.2023.105636>
- Yin, A., Harrison, T.M. (2000) Geologic Evolution of the Himalayan-Tibetan Orogen. *Annual Review of Earth and Planetary Sciences* 28, 211–280. <https://doi.org/10.1146/annurev.earth.28.1.211>
- Zhang, H.-F., Zhang, L., Harris, N., Jin, L.-L., Yuan, H. (2006) U–Pb zircon ages, geochemical and isotopic compositions of granitoids in Songpan-Garze fold belt, eastern Tibetan Plateau: constraints on petrogenesis and tectonic evolution of the basement. *Contributions to Mineralogy and Petrology* 152, 75–88. <https://doi.org/10.1007/s00410-006-0095-2>
- Zhang, H., Tian, S., Wang, D., Li, X., Liu, T., Zhang, Y., Fu, X., Hao, X., Hou, K., Zhao, Y., Qin, Y. (2021) Lithium isotope behavior during magmatic differentiation and fluid exsolution in the Jiajika granite–pegmatite deposit, Sichuan, China. *Ore Geology Reviews* 134, 104–139. <https://doi.org/10.1016/j.oregeorev.2021.104139>
- Zhao, H., Chen, B., Huang, C., Bao, C., Yang, Q., Cao, R. (2021) Geochemical and Sr–Nd–Li isotopic constraints on the genesis of the Jiajika Li-rich pegmatites, eastern Tibetan Plateau: implications for Li mineralization. *Contributions to Mineralogy and Petrology* 177, 4. <https://doi.org/10.1007/s00410-021-01869-3>
- Zheng, Y., Xu, Z., Li, G., Lian, D., Zhao, Z., Ma, Z., Gao, W. (2020) Genesis of the Markam gneiss dome within the Songpan-Ganzi orogenic belt, eastern Tibetan Plateau. *Lithos* 362–363, 105475. <https://doi.org/10.1016/j.lithos.2020.105475>
- Zhou, M., Zhang, R., Hanchar, J.M., Xu, Z., Lu, J., Hu, H., Che, X., Zheng, B., Li, G. (2023) Unravelling the genetic relationship between pegmatites and granites in the Jiajika Li–Be polymetallic district, Songpan-Ganze Orogenic Belt, Southwestern China: Insights from monazite U–Pb geochronology and trace element geochemistry. *Ore Geology Reviews* 163, 105774. <https://doi.org/10.1016/j.oregeorev.2023.105774>
- Zhu, J., Zhu, W., Xu, Z., Zhang, R., Che, X., Zheng, B. (2023) The geochronology of pegmatites in the Jiajika lithium deposit, western Sichuan, China: Implications for multi-stage magmatic-hydrothermal events in the Songpan-Ganze rare metal metallogenic belt. *Ore Geology Reviews* 159, 105582. <https://doi.org/10.1016/j.oregeorev.2023.105582>